

MiR-20 promotes cartilage repair in knee osteoarthritis rats via BMP2/Smad1 signaling pathway

Zhili Zheng^{1#}, Dingnan Wang^{1#}, Weiping Zhang², Han Yu³, Yi Zhang⁴, Ting Feng¹, Xianggen Zhong^{1*}

¹ Chinese Medicine College, Beijing University of Chinese Medicine, Beijing, China.

² Department of Preventive Medicine, Jiangxi Provincial Hospital of Integrated Traditional Chinese and Western Medicine, China

³ School of Basic Medicine, Chengdu University of Traditional Chinese Medicine, Chengdu, China

⁴ Department of Ophthalmology, Guang'anmen Hospital, China Academy of Chinese Medical Sciences, Beijing, China

[#]Zhili Zheng and Dingnan Wang as co-first authors.

ARTICLE INFO

Original paper

Article history:

Received: January 12, 2023

Accepted: April 01, 2023

Published: November 30, 2023

Keywords:

Knee osteoarthritis, BMP2/Smad1 signaling pathway, miR-20b, articular cartilage

ABSTRACT

This study investigated the impact of miR-20b on knee osteoarthritis (OA) in rats through the regulation of the BMP2/Smad1 pathway. Thirty-six SD rats were randomly assigned to normal (n=12), model (n=12), and miR-20b mimics (n=12) groups. The normal group received standard feeding, while the model and miR-20b mimics groups underwent knee OA model induction. Following modeling, the model group received no intervention, while the miR-20b mimics group received intra-articular injections of miR-20b mimics daily for 2 weeks. BBB limb motor function scoring was conducted on days 1, 5, 7, and 14 post-modeling and samples were collected after the 2-week intervention. Immunohistochemistry revealed decreased positive expressions of BMP2 and Smad1 in both model and miR-20b mimics groups compared to the normal group (P<0.05). However, the miR-20b mimics group exhibited significantly increased BMP2 and Smad1 expressions (P<0.05). miR-20b expression was markedly reduced in both model and miR-20b mimics groups compared to the normal group, with a significant elevation in the miR-20b mimics group versus the model group (P<0.05). ELISA demonstrated reduced COMP and CTX-II in both model and miR-20b mimics groups versus the normal group (P<0.05), with a significant increase in the miR-20b mimics group compared to the model group (P<0.05). Furthermore, the relative expression levels of BMP2 and Smad1 proteins decreased in both model and miR-20b mimics groups versus the normal group (P<0.05), but increased significantly in the miR-20b mimics group compared to the model group (P<0.05). In conclusion, miR-20b enhances cartilage repair and improves articular function in knee OA rats by upregulating the BMP2/Smad1 signaling pathway.

Doi: <http://dx.doi.org/10.14715/cmb/2023.69.12.40>

Copyright: © 2023 by the C.M.B. Association. All rights reserved. 

Introduction

Knee osteoarthritis (OA) stands as a prevalent and clinically significant inflammatory disease, primarily characterized by the progressive degradation of articular cartilage and subchondral bone (1, 2). The ramifications of knee OA extend beyond mere physical discomfort, often giving rise to persistent pain, rest-related discomfort, and limitations in the flexion and extension of the knee joint, collectively exerting a profound impact on the overall quality of life for affected individuals (3, 4). With its escalating incidence year by year, particularly in the middle-aged and elderly demographic, knee OA poses a growing health concern, exacerbated by the global trend of population aging (5).

Numerous studies (6, 7) have underscored the pivotal role of repairing articular cartilage and subchondral bone in mitigating the pathogenesis of knee OA. The challenge lies in the clinical realm, where effective strategies for enhancing the repair of articular cartilage and subchondral bone in knee OA patients have remained elusive. Micro ribonucleic acid (miR)-20b emerges as a key player in the intricate regulatory network governing the pathophysio-

logy of knee OA. Simultaneously, the morphogenetic protein 2 (BMP2)/Smad1 signaling pathway, a vital conduit for cellular signal transduction, is recognized for its central regulatory effects on chondrocyte processes, including proliferation, apoptosis, and necrosis (8, 9). Both miR-20b and the BMP2/Smad1 pathway are implicated as core contributors to the multifaceted pathogenesis of knee OA.

In light of this backdrop, the primary objective of this study is to delve into the nuanced interplay between miR-20b and the BMP2/Smad1 signaling pathway in the context of knee OA. By dissecting the molecular mechanisms and functional consequences of miR-20b modulation, particularly concerning its regulatory influence on the BMP2/Smad1 pathway, we aim to advance our understanding of the molecular intricacies underpinning knee OA pathogenesis. This investigation is positioned to bridge existing knowledge gaps and provide valuable insights into potential therapeutic avenues for knee OA.

As knee OA continues to impose a substantial burden on affected individuals and the healthcare system at large, a comprehensive exploration of miR-20b and its interconnection with the BMP2/Smad1 pathway holds the promise

* Corresponding author. Email: zhongxg@bucm.edu.cn

of unveiling novel targets for intervention. The outcomes of this study are anticipated to not only deepen our comprehension of the molecular underpinnings of knee OA but also pave the way for the development of targeted therapeutic strategies aimed at enhancing articular cartilage and subchondral bone repair in a clinical setting. Through rigorous experimentation and meticulous analysis, we aspire to contribute meaningfully to the growing body of knowledge dedicated to unraveling the complexities of knee OA pathogenesis and identifying avenues for improved clinical management.

Materials and Methods

Animal grouping

A total of 36 Sprague Dawley (SD) rats weighing about 200 g were randomly divided into the normal group (n=12), model group (n=12) and miR-20b mimics group (n=12), and they were used for the experiment after 7 days of adaptive feeding in the laboratory animal center. This study was approved by the Animal Ethics Committee of Chinese Medicine College, Beijing University of Chinese Medicine Animal Center.

Experimental reagents and instruments

MiR-20b mimics (GeneChem, Shanghai, China), primary antibodies: anti-BMP2 antibody (Abcam, Cambridge, MA, USA) and anti-Smad1 antibody (Abcam, Cambridge, MA, USA), immunohistochemistry kit (MXB Biotechnologies, Fuzhou, China), enzyme-linked immunosorbent assay (ELISA) kit (BOSTER, Wuhan, China), quantitative polymerase chain reaction (qPCR)-related kits (Vazyme, Nanjing, China), optical microscope (Leica DMI 4000B/DFC425C, Wetzlar, Germany) and fluorescence qPCR instrument (ABI 7500, Applied Biosystems, Foster City, CA, USA).

Establishment of rat models of knee osteoarthritis

The rats were anesthetized with 3% pentobarbital sodium (injection volume: 5 mL/kg). After successful anesthesia, local disinfection and knee joint exposure were conducted. Then the rats were injected with 0.1 mL of 2% papain and 0.05 mL of 0.05 mmol/L L-cysteine into the knee joint, which was repeated 4 days later to establish rat models of knee osteoarthritis.

Treatment in each group

Normal group was fed normally without any treatment. In the model group and miR-21 mimics group, the knee osteoarthritis models were prepared using the above method, and the same amount of normal saline and 10 μ M of miR-21 mimics were injected into the joint cavity after operation, respectively. The rats in each group underwent Basso, Beattie and Bresnahan (BBB) limb motor function scoring on the postoperative 1st, 5th, 10th and 14th day, and samples were obtained at 2 weeks after intervention.

Sampling

After successful anesthesia, 6 rats were randomly selected from each group, and the knee articular cartilage tissues were soaked in 4% paraformaldehyde for 48 h and then in EDTA (ethylenediaminetetraacetic acid) decalcification solution (Thermo Fisher Scientific, Waltham, MA, USA) for decalcification for immunohistochemical detec-

tion. Thereafter, the knee articular cartilage tissues of the remaining rats were taken and stored in an ultra-low temperature refrigerator for Western blotting (WB), qPCR and ELISA.

Hematoxylin and eosin (H&E) staining

The tissues embedded by paraffin in advance were cut into 5- μ m thick sections, placed into warm water at 42°C for section flattening, fishing and baking, and prepared into paraffin-embedded tissue sections. Next, these paraffin-embedded tissue sections were sequentially put into a xylene solution and gradient alcohol for soaking, and conventional deparaffinization was carried out until water was added. Subsequently, H&E staining kit was applied to stain the sections in hematoxylin dye for 5 min and then in pure water for 10 min. Finally, they underwent color separation with 95% ethanol for 5 s, transparentization with xylene for 10 s, and mounting by neutral gum.

Markin's scoring

Cartilage tissue morphology, staining and tide line in each group were evaluated by Markin's scoring. The higher Markin's score indicates more obvious degeneration of articular cartilages.

Immunohistochemistry

The tissues embedded by paraffin in advance were cut into 5 μ m-thick sections, followed by section flattening, fishing and baking in warm water at 42°C, and prepared into paraffin-embedded tissue sections. Then these sections were sequentially put into xylene solution and gradient alcohol for soaking, and conventional deparaffinization was carried out until water was added. After that, the sections were immersed in citric acid buffer solution, placed in a microwave oven for repeatedly heating for 3 times, with 3 min each time, and braised for 5 min, so as to fully carry out antigen repair. Following rinsing, endogenous peroxidase blockers were dripped onto the samples, reacted for 10 min and then rinsed again. Then goat serum was dripped for sealing for 20 min, and after the goat serum sealing solution was removed, anti-Bax primary antibody (1:200) and anti-Bcl-2 primary antibody (1:200) were added and placed in a refrigerator at 4°C overnight. On the next day, the samples were rinsed and dripped with secondary antibody solution for reaction for 10 min. After fully rinsing, the streptavidin-peroxidase solution was added for a reaction for 10 min. Finally, diaminobenzidine (DAB) was added dropwise for color development, and hematoxylin was applied to re-stain the nucleus, followed by mounting and observation.

ELISA

The abdominal aorta blood was put into a high-speed centrifuge for centrifugation at 14,000 g for 10 min, and the supernatant was taken. Afterward, according to the instructions of the ELISA kit, samples were sequentially loaded, standards, biotinylated antibody working fluid and enzyme conjugate working fluid were added, and plates were washed. At last, the samples were put into an enzyme labeling instrument for detection at 450 nm.

QPCR

The total RNA in tissue samples was extracted first, and then reversely transcribed into complementary deoxy-

Table 1. Primer sequence.

Name	Primer sequence
MiR-20b	Forward primer: 5'TACCATTGGCCAATGCCTGGTTA3'
	Reverse primer: 5'CAATTCCGGCCGGTTATAATGCT3'
GAPDH	Forward primer: 5'ACGGCAAGTTCAACGGCACAG3'
	Reverse primer: 5'GAAGACGCCAGTAGACTCCACGAC3'

ribose nucleic acid (cDNA). The reaction system was 20 μ L. Reaction conditions: reaction at 50°C for 2 min, pre-denaturation at 95°C for 10 min, denaturation at 95°C for 10 s and annealing at 50°C for 30 s for 45 cycles. With glyceraldehyde 3-phosphate dehydrogenase (GAPDH) as an internal reference, the relative expression of mRNA was calculated. Specific primer sequences are shown in Table 1.

WB

The lysate was added to the cartilage tissues preserved at ultra-low temperature, subjected to an ice bath for 1 h, and centrifuged for 10 min (1,4000 g) in a centrifuge, followed by protein quantification using bicinchoninic acid (BCA) method (Pierce, Rockford, IL, USA). The absorbance value and the standard curve obtained by protein detection through a microplate reader were utilized for the calculation of the protein concentration in tissues. Then protein denaturation was carried out, sodium dodecyl sulphate-polyacrylamide gel electrophoresis (SDS-PAGE) was conducted to separate the proteins in tissue samples, and the position of Marker proteins was observed. When Marker proteins were at the bottom of the glass plate in a straight line, the electrophoresis was terminated. Subsequently, the proteins were transferred onto polyvinylidene fluoride (PVDF) membrane, and anti-BMP2 primary antibody (1:1000), anti-ROCK1 primary antibody (1:1000) and secondary antibody (1:1000) were sequentially added after the blocking solution was added for 1.5 h of reaction. After rinsing, the color was fully developed in the dark with the chemiluminescent reagent for 1 min.

Statistical analysis

Data were statistically processed using Statistical Product and Service Solutions (SPSS) 20.0 software (IBM, Armonk, NY, USA) and expressed as mean \pm standard deviation. When the data met the normal distribution and the homogeneity of variance, a t-test was performed. Otherwise, nonparametric tests were performed. $P < 0.05$ represented a statistically significant difference.

Results

Limb motor function of rats in each group

As shown in Figure 1, compared with normal group, model group and miR-20b mimics group had a notably reduced BBB limb motor function score, with statistically significant differences ($P < 0.05$). In comparison with that in model group, the BBB limb motor function score in miR-20b mimics group was significantly increased from the 7th day after intervention, showing a statistically significant difference ($P < 0.05$). It was discovered that the articular surface in normal group was smooth and flat, with normal morphology, clear structure and no obvious damage. In model group, the articular surface was not smooth and uneven, and more articular cartilage fractures, morpholo-

gical disorders and structural damages could be observed. Moreover, the articular surface in miR-20b mimics group was slightly damaged and smoother, and its morphology and structure were markedly improved in contrast to that in model group.

Markin's score

As displayed in Figure 2, Markin's score in normal group was overtly lower than that in model group and miR-20b mimics group, and the differences were statistically significant ($p < 0.05$). In comparison with model group, miR-20b mimics group has an obviously reduced Markin's score, showing a statistically significant difference ($P < 0.05$).

Immunohistochemistry results

As shown in Figure 3, medium brown indicates a positive expression. The positive expression levels of BMP2

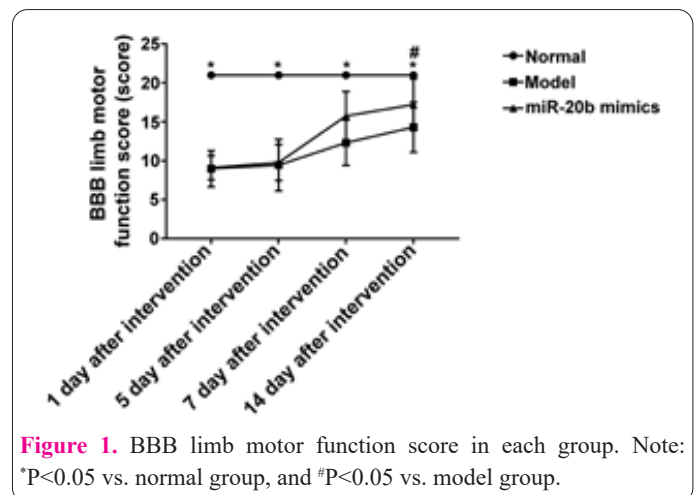


Figure 1. BBB limb motor function score in each group. Note: * $P < 0.05$ vs. normal group, and # $P < 0.05$ vs. model group.

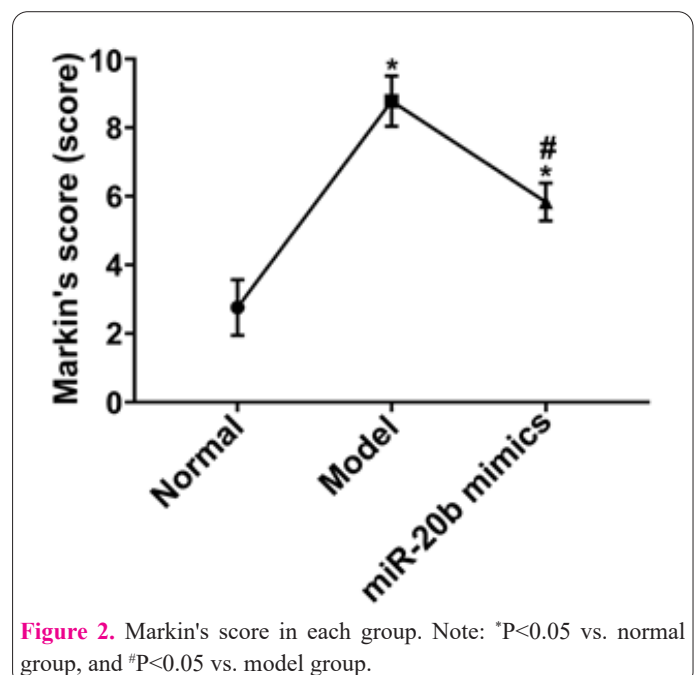


Figure 2. Markin's score in each group. Note: * $P < 0.05$ vs. normal group, and # $P < 0.05$ vs. model group.

and Smad1 were higher in the normal group than those in the other two groups. The statistical analysis results manifested that in contrast to that in the normal group, the positive expression level of BMP2 in the other two groups was markedly reduced, with statistically significant differences ($P < 0.05$). In addition, the positive expressions of BMP2 and Smad1 in the miR-20b mimics group were markedly increased in comparison with those in the model group, displaying statistically significant differences ($P < 0.05$).

MRNA expression detected via qPCR

The results revealed that the expression of miR-20b was higher in normal group than that in the other two groups. Compared with that in normal group, the expression of miR-20b in the other two groups was prominently reduced, with statistically significant differences ($P < 0.05$). Besides, in comparison with model group, miR-20b mimics group exhibited an overtly raised expression of miR-20b, showing a statistically significant difference ($P < 0.05$) (Figure 4).

ELISA detection results

As displayed in Figure 5, it was illustrated that the content of cartilage oligomeric matrix protein (COMP) and C-telopeptide of type II collagen (CTX-II) in the cartilage tissues in the other two groups were evidently reduced compared with that in normal group ($P < 0.05$), and the differences were statistically significant. In addition, the content of COMP and CTX-II was increased prominently in miR-20b mimics group compared with that in

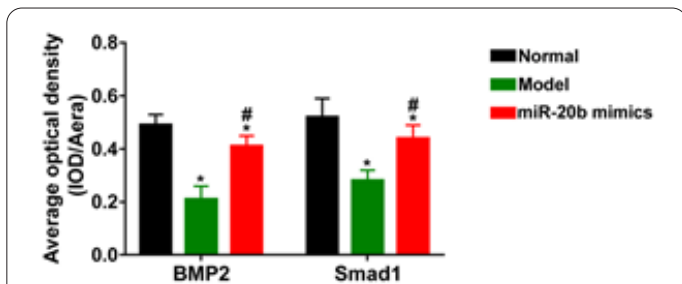


Figure 3. Immunohistochemistry results. The average optical density of the positive expression in each group. * $P < 0.05$ vs. normal group, and # $P < 0.05$ vs. model group.

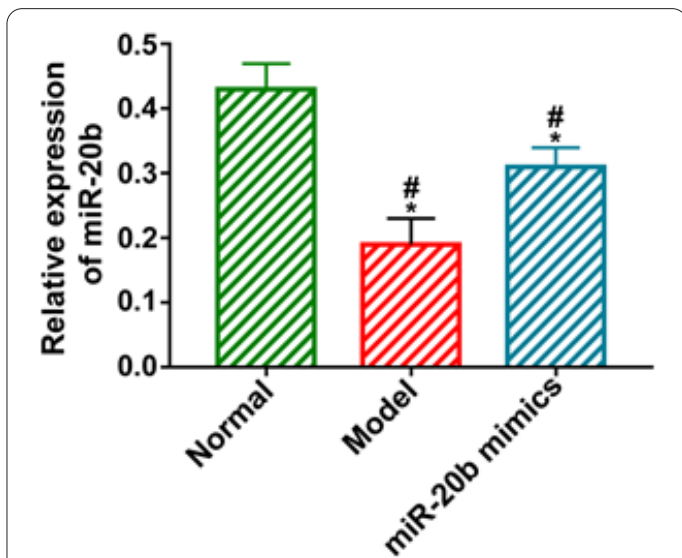


Figure 4. Relative expression of miR-20b in each group Note: * $P < 0.05$ vs. normal group, and # $P < 0.05$ vs. model group.

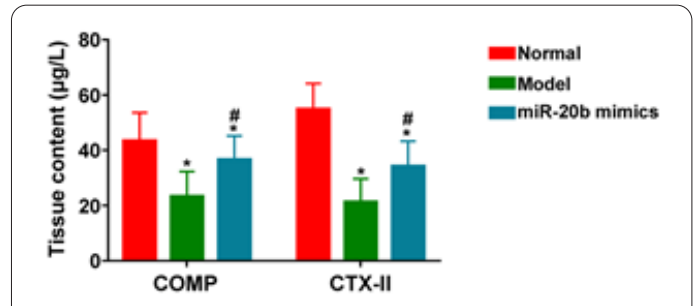


Figure 5. ELISA detection results. Note: * $P < 0.05$ vs. normal group, and # $P < 0.05$ vs. model group.

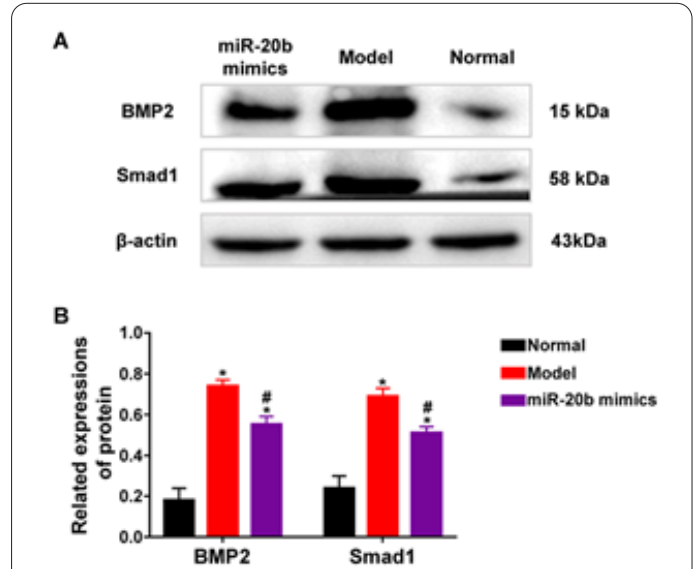


Figure 6. Related protein expressions detected via WB. Note: (A) WB detection. (B) Relative expression of proteins in each group. * $P < 0.05$ vs. normal group, and # $P < 0.05$ vs. model group.

model group ($P < 0.05$), displaying a statistically significant difference.

Related protein expressions detected via WB

Medium brown represented the positive expression. According to the results, the relative expression levels of BMP2 and Smad1 proteins in normal group were higher than those in the other two groups (Figure 6A). The statistical analysis results (Figure 6B) illustrated that in contrast to that in normal group, the relative expression levels of proteins in the other two groups were markedly reduced, with statistically significant differences ($P < 0.05$). In addition, the relative expression levels of BMP2 and Smad1 proteins in miR-20b mimics were markedly increased in comparison with those in model group, displaying statistically significant differences ($P < 0.05$).

Discussion

Knee osteoarthritis is the most common inflammatory disease in middle-aged and elderly patients as well as the most common cause of knee joint pain, knee joint dysfunction and knee joint deformity in these patients (10, 11). It is currently held that the pathological mechanism of knee osteoarthritis is very complex, involving knee inflammation, degeneration of articular cartilage and subchondral bone, apoptosis of articular cartilage, fibrosis and many other pathological reactions and related mechanisms (12, 13). A study (14) has revealed that the degeneration

of articular cartilage and subchondral bone is a pathological change during knee osteoarthritis, and an important pathological factor leading to joint pain, deformity, hyperostosis and limited joint activity in patients. Hence, further research on the degeneration of articular cartilage and subchondral bone during knee osteoarthritis is critical for the clarification of the pathological mechanism and treatment of knee osteoarthritis. Besides, it has been confirmed by studies (15, 16) that the destruction of articular cartilage and subchondral bone after knee osteoarthritis exerts crucial effects on the occurrence, development rehabilitation and prognosis of knee osteoarthritis. Further studies (17, 18) have confirmed that the BMP2/Smad1 signaling pathway, as a vital signaling pathway in the body, effectively facilitates the repair and regeneration of articular cartilage and subchondral bone. COMP and CTX-II, as the main components of articular cartilage and subchondral bone, are efficacious markers reflecting the state of articular cartilage and subchondral bone during osteoarthritis. In the meantime, they are important downstream effector molecules of the BMP2/Smad1 signaling pathway and are modulated by this pathway. The activated BMP2/Smad1 signaling pathway contributes to the maintenance of the normal physiological state and function of articular cartilage and subchondral bone by COMP and CTX-II. In addition, COMP and CTX-II are key members of the miRNA family that play important regulatory roles in multiple downstream signaling pathways, so as to modulate cell proliferation and apoptosis as well as the regeneration and repair of articular cartilage and subchondral bone (19, 20). The results of this study demonstrated that the content of COMP and CTX-II in the knee joint of knee osteoarthritis rats was decreased prominently, and the expressions of BMP2 and Smad1, vital molecules in the BMP2/Smad1 signaling pathway, were reduced significantly, suggesting that the BMP2/Smad1 signaling pathway is inhibited in the knee joint of knee osteoarthritis rats. This may be the major cause for the notable decrease in the content of COMP and CTX-II as well as the morphological change and functional limitation of the knee joint. Moreover, intervention with miR-20b mimics was carried out in this study to further explore the regulatory role of miR-20b in knee osteoarthritis. It was discovered that miR-20b mimics overtly stimulated the expressions of BMP2, Smad1, COMP and CTX-II after elevating the expression of miR-20b, indicating that miR-20b promotes the repair and regeneration of articular cartilage and subchondral bone, and simultaneously improves the tissue morphology and limb function of knee osteoarthritis rats through distinctively up-regulating the BMP2/Smad1 signaling pathway.

Conclusions

In conclusion, miR-20b contributes to cartilage repair and improves articular function in knee osteoarthritis rats through up-regulating the BMP2/Smad1 signaling pathway.

Abbreviations

Micro ribonucleic acid (miR); bone morphogenetic protein 2 (BMP2); Basso, Beattie and Bresnahan (BBB); hematoxylin and eosin (H&E); cartilage oligomeric matrix protein (COMP); C-telopeptide of type II collagen (CTX-II); enzyme-linked immunosorbent assay (ELISA); Western blotting (WB).

Acknowledgments

The authors thank the staff of the Animal Experimental Center of Beijing University of Chinese Medicine (Beijing, China) for the technical support. In addition, we would like to thank Xiulan Deng for her guidance on scientific thinking, and express special thanks to HY for his continued support and care. This study was supported by National Natural Science Foundation of China (82374312).

Conflict of Interest

The authors declared no conflict of interest.

References

- Oo WM, Linklater JM, Hunter DJ. Imaging in knee osteoarthritis. *Curr Opin Rheumatol* 2017; 29(1): 86-95.
- Shirinsky IV, Kalinovskaya NY, Filatova K, Shirinsky VS. Pleiotropic Effects of Comarum palustre L. in Patients with Osteoarthritis and Diabetes Mellitus with High Comorbidity Burden: An Exploratory Study. *Altern Ther Health M* 2021; 27(80-84).
- Kujala UM, Kaprio J, Sarna S. Osteoarthritis of weight bearing joints of lower limbs in former elite male athletes. *Bmj-Brit Med J* 1994; 308(6923): 231-234.
- Li T, Guo M, Zhang W. Comparison of Therapeutic Effects of Topical Application of Diclofenac Sodium Nanoparticles and Conventional Placebo on Knee Osteoarthritis. *Cell Mol Biol* 2022; 68(3): 171-178.
- Gurudut P, Jaiswal R. Comparative Effect of Graded Motor Imagery and Progressive Muscle Relaxation on Mobility and Function in Patients with Knee Osteoarthritis: A Pilot Study. *Altern Ther Health M* 2022; 28(3): 42-47.
- Zamli Z, Robson BK, Tarlton JF, et al. Subchondral bone plate thickening precedes chondrocyte apoptosis and cartilage degradation in spontaneous animal models of osteoarthritis. *Biomed Res Int* 2014; 2014: 606870.
- Wu T. The effect of Psidium guajava hydroalcoholic extract on reducing the expression of Resistin and TNF-alpha genes in articular chondrocytes of patients with knee osteoarthritis. *Cell Mol Biol* 2021; 67(6): 74-81.
- Valdes AM, Spector TD, Tamm A, et al. Genetic variation in the SMAD3 gene is associated with hip and knee osteoarthritis. *Arthritis Rheum* 2010; 62(8): 2347-2352.
- Sharma AC, Srivastava RN, Srivastava SR, Parmar D, Singh A, Raj S. Association between Single Nucleotide Polymorphisms of SMAD3 and BMP5 with the Risk of Knee Osteoarthritis. *J Clin Diagn Res* 2017; 11(6): GC1-GC4.
- Liu B, Zhao B, Xiao Q. Effect of Fibular Osteotomy with Joint Debridement on Pain and Range of Motion in Patients with Knee Osteoarthritis. *Altern Ther Health M* 2022; 28(5): 44-48.
- Felson DT, Naimark A, Anderson J, Kazis L, Castelli W, Meenan RF. The prevalence of knee osteoarthritis in the elderly. The Framingham Osteoarthritis Study. *Arthritis Rheum* 1987; 30(8): 914-918.
- Jonsson H, Manolescu I, Stefansson SE, et al. The inheritance of hand osteoarthritis in Iceland. *Arthritis Rheum* 2003; 48(2): 391-395.
- Ingvarsson T, Stefansson SE, Hallgrimsdottir IB, et al. The inheritance of hip osteoarthritis in Iceland. *Arthritis Rheum* 2000; 43(12): 2785-2792.
- Hwang HS, Kim HA. Chondrocyte Apoptosis in the Pathogenesis of Osteoarthritis. *Int J Mol Sci* 2015; 16(11): 26035-26054.
- D'Lima DD, Hashimoto S, Chen PC, Colwell CJ, Lotz MK. Human chondrocyte apoptosis in response to mechanical injury. *Osteoarthr Cartilage* 2001; 9(8): 712-719.

16. Aigner T, Kim HA. Apoptosis and cellular vitality: issues in osteoarthritic cartilage degeneration. *Arthritis Rheum* 2002; 46(8): 1986-1996.
17. Wu Q, Kim KO, Sampson ER, et al. Induction of an osteoarthritis-like phenotype and degradation of phosphorylated Smad3 by Smurf2 in transgenic mice. *Arthritis Rheum* 2008; 58(10): 3132-3144.
18. Otsuki S, Hanson SR, Miyaki S, et al. Extracellular sulfatases support cartilage homeostasis by regulating BMP and FGF signaling pathways. *P Natl Acad Sci Usa* 2010; 107(22): 10202-10207.
19. Wang X, Lin B, Nie L, Li P. microRNA-20b contributes to high glucose-induced podocyte apoptosis by targeting SIRT7. *Mol Med Rep* 2017; 16(4): 5667-5674.
20. Guo S, Wang H, Luo Y, et al. Sp-1 Negatively Regulates miR-20b Expression in Macrophages. *Ann Clin Lab Sci* 2017; 47(6): 706-712.